Available online at www.sciencedirect.com

ScienceDirect

Ceramics International 40 (2014) 10217–10221

CERAMICS INTERNATIONAL

www.elsevier.com/locate/ceramint

Synthesis and characterization of ZnO NPs/reduced graphene oxide nanocomposite prepared in gelatin medium as highly efficient photo-degradation of MB

Majid Azarang[a,b,*], Ahmad Shuhaimi[a], Ramin Yousefi[c,**], A. Moradi Golsheikh[a], M. Sookhakian[a]

[a]Low Dimensional Materials Research Center, Department of Physics, Faculty of Science, University of Malaya, 50603 Kuala Lumpur, Malaysia
[b]Department of Physics, University of Sistan and Baluchestan, 98135-674 Zahedan, Iran
[c]Department of Physics, Masjed-Soleiman Branch, Islamic Azad University (I.A.U), Masjed-Soleiman, Iran

Received 14 February 2014; received in revised form 25 February 2014; accepted 25 February 2014
Available online 7 March 2014

Abstract

ZnO nanoparticles (NPs) were decorated on a graphene oxide (GO) sheet via the sol–gel method in a gelatin medium. Long-chain gelatin compounds were utilized to terminate the growth of the ZnO-NPs on GO and stabilize them. The obtained products were post-annealed at 400 °C to remove the gelatin and produce a reduced graphene oxide (RGO) sheet. Microscopic studies showed that the NPs were dispersed on the GO sheet. They had a spherical shape and a size of approximately 19 nm. In addition, these studies revealed that the NPs were single crystals. The X-ray diffraction pattern of the NPs indicated a hexagonal (wurtzite) structure. The results of Fourier transform infrared spectroscopy (FTIR) revealed that the GO sheet was transformed into RGO by the post-annealing process. The obtained ZnO-NPs/RGO nanocomposite was used as photocatalyst to remove methylene blue (MB). Observations showed that the efficiency of the photocatalyst activity of the ZnO NPs was significantly increased by RGO.

Keywords: A. Sol–gel process; B. Nanocomposites; ZnO NPs; Reduced graphene oxide; Photocatalyst

1. Introduction

Currently, organic dyes and their effluents have become one of the main sources of water pollution; these organic dyes escape from the traditional wastewater treatment plants and remain in the water because of their high stability against light, temperature, chemicals, and microbial attack [1,2]. It has been proven that many semiconductors can be used in the photo-degradation of recalcitrant organic pollutants [3–5]. Among these, ZnO, which is a semiconductor that is widely used as photonic crystals, photocatalysts, light-emitting diodes, sensors, and electroluminescent materials [6], has been given attention because of its large band gap (3.3 eV), and other beneficial characteristics. For example, ZnO is an environmental friendly material and can be used in many applications, including transparent conductive coatings [7], electrodes for dye-sensitized solar cells [8], gas sensors [9], field emission materials [10], and photocatalyst materials [11]. In addition, apart from the technological significance of ZnO nanostructures, their quasi-one-dimensional structure, with diameters in the range of tens of nanometers to hundreds of nanometers, makes them interesting from a scientific point of view. In this size range, they are expected to possess interesting physical properties and pronounced coupling quite different from their bulk counterpart [12]. Therefore, ZnO can be used as a photocatalyst material to remove organic dyes from wastewater with high efficiency. A photocatalyst is also called a photo-chemical catalyst, and its function is similar to that of

*Corresponding author at: Low Dimensional Materials Research Center, Department of Physics, Faculty of Science, University of Malaya, 50603 Kuala Lumpur, Malaysia. Tel.:+60 123161935; fax: +60 379674146.
**Corresponding author. Tel.: +989166224993, +986813330093.
E-mail addresses: azarangmajid@gmail.com (M. Azarang), Yousefi.ramin@gmail.com (R. Yousefi).

http://dx.doi.org/10.1016/j.ceramint.2014.02.109
0272-8842

chlorophyll in photosynthesis. In a photocatalytic system, a photo-induced molecular transformation or reaction takes place at the surface of the catalyst. A basic mechanism of a photocatalytic reaction is the generation of an electron–hole pair, which can be described as follows. When a photocatalyst is illuminated by a light stronger than its band gap energy, electron–hole pairs diffuse out to the surface of the photocatalyst and participate in a chemical reaction with the electron donor and acceptor. Those free electrons and holes transform the surrounding oxygen or water molecules into hydroxyuracil (OHU) free radicals with super strong oxidation. However, this super strong oxidation of the OHU free radicals generated on the surface of ZnO nanoparticles makes OHU free radicals harmful to human beings when used in cosmetics. Therefore, it is necessary to modify the application of ZnO nanoparticles as a photocatalyst material to obtain a good UV shielding ability. Recently, graphene, one of the members of the carbon family with interesting properties, has generated increasing interest both in fundamental science and for a wide range of potential applications because of its excellent electronic properties, superior chemical stability, and high specific surface area [13]. Similar to carbon nanotubes (CNTs), graphene can also act as an excellent electron-acceptor/transport material and attempts to combine a semiconductor oxide photocatalyst and graphene have been reported in efforts to obtain hybrid materials with superior photocatalytic performance [14].

We believe that the sol–gel method is the best method to obtain a uniform distribution of nanomaterials in semiconductors. In addition, using a suitable polymer agent such as gelatin can improve the quality of the final products. Therefore, in this study, a simple sol–gel method was used to synthesize ZnO nanoparticles with a narrow size distribution that were decorated on a reduced graphene oxide (RGO) sheet in a gelatin medium. Gelatin was used as a polymerization agent, and it served as a terminator for the growth of the ZnO-NPs because it expanded during the calcination process, which prevented the particles from coming together easily. Then, the obtained products were used as photocatalyst materials to remove methylene blue (MB), which is one of the dye materials.

2. Experimental

First, graphene oxide (GO) was synthesized using the Hummers method [15]. Then, the ZnO NPs to be decorated on the GO sheet were synthesized using a simple sol–gel method in a gelatin medium used as a polymerization agent. In this synthesis, 5 g of ZnO (NPs)/GO (15%), analytical grade zinc nitrate hexahydrate $Zn(NO_3)_2 \cdot 6H_2O$, gelatin (type B from bovine skin), and distilled water were used as the starting materials. All the materials used were purchased from Sigma-Aldrich. First, a gelatin solution was prepared by adding gelatin (1.25 g) to 20 ml of distilled water at 60 °C. The zinc nitrate (4.46 g) was dissolved separately in a minimal amount of distilled water at room temperature, and 0.669 g of GO was added to this zinc nitrate solution. Finally, the obtained solution was added to the gelatin solution. After this, the compound solutions were stirred and heated at 80 °C until a gel with a dark brown color was obtained. The gel was calcined at 300 °C for 1 h, at a heating rate of 2 °C/min. Finally, a post-annealing process was performed for 2 h at 400 °C under an Ar gas atmosphere to remove the gelatin material and obtain the final nanocomposite. The resulting powder was characterized using several tools to check its quality. The crystal phase, morphology, and microstructure of the product were characterized using X-ray powder diffraction, XRD (Philips, X'pert, system using CuKα radiation), field emission scanning electron microscopy (FESEM, FEI Nova NanoSEM 400 operated at 10.0 kV), transmission electron microscopy (TEM, Hitachi H-7100), and Fourier transform infrared spectrometry (FTIR, Perkin-Elmer System 2000 series spectrophotometer (USA) by the KBr method). In addition, UV–visible spectroscopy (Perkin-Elmer spectrometer) was applied to consider the optical properties.

The photocatalytic performance of the as-prepared samples was evaluated using the photocatalytic degradation of MB under UV light irradiation. Here, 10 mg of the obtained material was dispersed in 30 ml of the MB aqueous solution (10 mg/l). The mixed suspension was magnetically stirred for 30 min in dark to reach an adsorption–desorption equilibrium. Under ambient conditions and stirring, the mixed suspension was exposed to UV irradiation produced by a 500 W high-pressure Hg lamp with the main wave crest at 365 nm for different times (0–180 min). At certain time intervals, 2.5 ml of the mixed suspension was extracted and centrifuged to remove the photocatalyst. The degradation process was monitored by measuring the absorption of MB in the filtrate at 664 nm using a UV–vis absorption spectrometer.

3. Results and discussion

Fig. 1 shows FESEM and TEM images of the ZnO NPs that were decorated on the GO sheet. It can be seen in the FESEM image (Fig. 1(a)) that the entire area of the GO sheet is covered by the ZnO NPs. The inset of Fig. 1(a) shows that the ZnO NPs have a spherical shape. The TEM image reveals that the ZnO NPs are dispersed on the GO (Fig. 1(b)). In addition, the TEM image shows an average particle size of approximately 19 ± 2 nm for the NPs. The inset of Fig. 1(b) shows an HRTEM image of a single nanoparticle. As can be seen, the nanoparticle is a single crystal with a high crystal quality, and there is no defect from a stacking fault. In addition, the HRTEM image shows that the lattice distance is approximately 0.26 nm, which is consistent with the distance along the *c*-axis of a bulk wurtzite ZnO crystal. Therefore, based on the HRTEM image, the nanoparticles were grown along the [001] direction without any defects.

The XRD patterns of the obtained products are shown in Fig. 2. The XRD pattern of GO indicates an intense and sharp diffraction peak at $2\theta = 10.6^\circ$, attributed to the (001) lattice plane corresponding to a *d*-spacing of 0.83 nm. This is consistent with the lamellar structure of GO. In addition, Fig. 2 shows the XRD pattern of the ZnO-NPs that are decorated on the GO sheet. All the detectable peaks can be

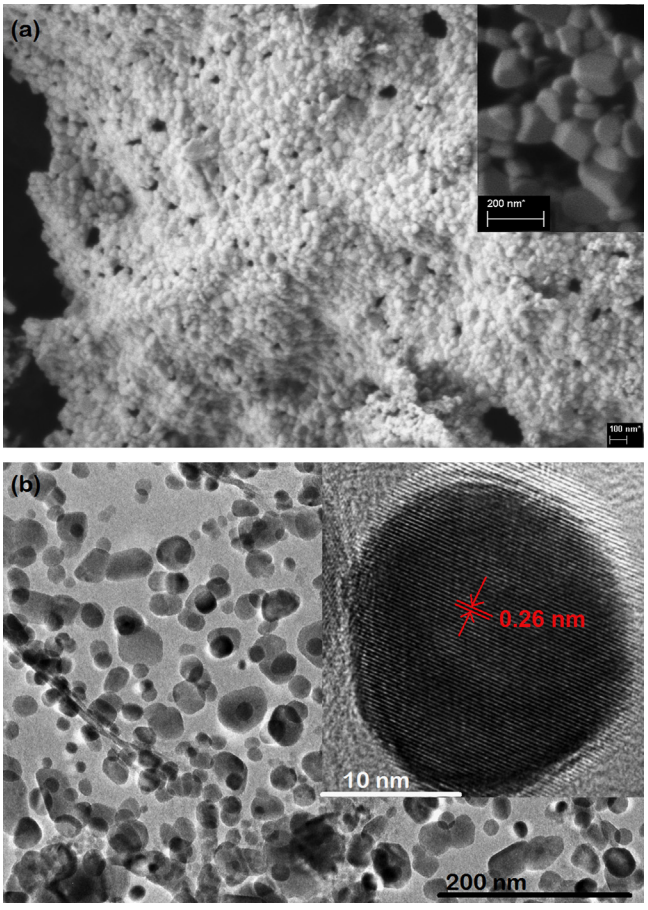

Fig. 1. (a) FESEM image of ZnO-NPs on the GO sheet. The inset shows ZnO nanoparticles that were deposited on the GO. (b) TEM image of dispersed ZnO NPs on the GO. The inset shows an HRTEM image of a single ZnO nanoparticle.

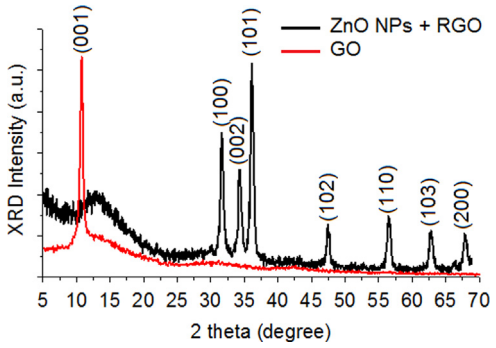

Fig. 2. XRD patterns of the GO sheet and ZnO-NPs/GO composite.

indexed to the ZnO wurtzite structure (Ref. code: 00-036-1451). It can be seen that there are no peaks from GO or other impurities in the XRD pattern of the ZnO NPs. This could be due to the transformation of GO to RGO, with the RGO peaks not appearing because of the strong peak of the ZnO NPs in the XRD pattern. However, additional characterization is needed to explain this phenomenon.

Fig. 3 shows the FTIR spectra of the pristine GO and ZnO-NPs/GO nanocomposite. In the FTIR spectrum for GO, the broad peak centered at 3190 cm^{-1} is attributed to the O–H

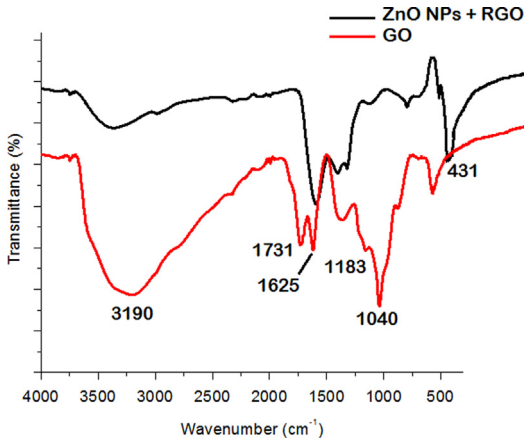

Fig. 3. FTIR spectra of the GO sheet and ZnO-NPs/RGO composite.

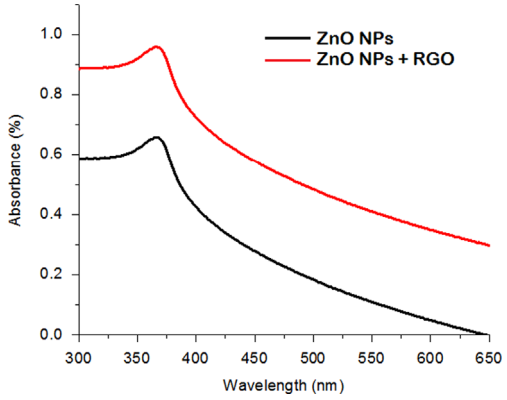

Fig. 4. UV–vis absorption spectra of the GO sheet and ZnO-NPs/RGO composite.

stretching vibrations, and the peaks at 1731, 1625, 1183, and 1040 cm^{-1} are assigned to the C=O stretching, sp^2-hybridized C=C group, O–H deformation, C–OH stretching, and C–O stretching, respectively [16]. In contrast, the peaks at 1731 and 1183 cm^{-1} are missing from the FTIR spectrum of the ZnO-NPs/GO nanocomposite, which indicates the reduction of GO and its transformation into RGO [17–18]. In fact, the post-annealing process at 400 °C not only removed the gelatin but also caused the transformation of GO to RGO. Therefore, the obtained nanocomposite consisted of ZnO NPs decorated on an RGO sheet. The broad peak at 3250 cm^{-1} in the FTIR spectrum of the ZnO-NPs/GO nanocomposite might be attributed to the O–H stretching vibration of absorbed water molecules. In addition, the FTIR spectrum of ZnO-NPs/RGO shows a peak at 431 cm^{-1}. The band at 431 cm^{-1} corresponds to the E_2 mode of hexagonal ZnO (Raman active) [19].

UV–vis absorption spectra of ZnO NPs and ZnO-NPs/RGO at room temperature are shown in Fig. 4. These spectra reveal a characteristic absorption peak for ZnO at a wavelength of 360 for both samples, which can be assigned to the intrinsic band-gap absorption of ZnO, owing to the electron transitions from the valence band to the conduction band ($O_{2p} \rightarrow Zn_{3d}$) [20]. As can be seen, the peak position of the UV–vis spectrum of ZnO NPs has not been affected by the graphene. However, it is

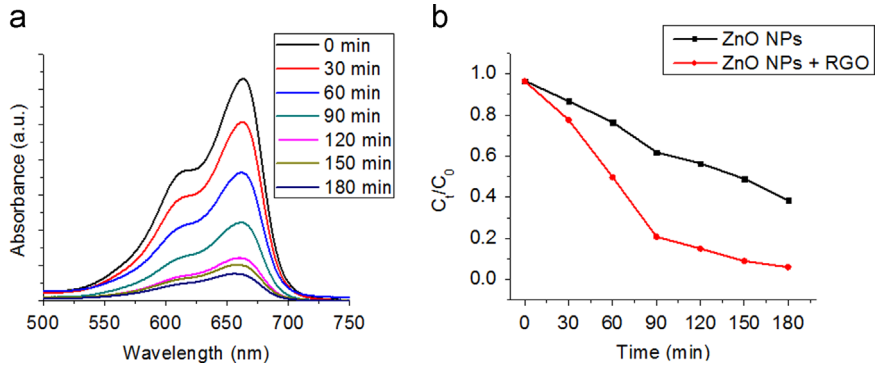

Fig. 5. (a) The UV–vis absorbance of MB over time during photocatalytic degradation under UV light irradiation using ZnO-NPs/RGO. (b) Photocatalytic degradation of MB by ZnO NPs and ZnO-NPs/RGO under UV light irradiation.

observed that the absorbance of the ZnO-NPs/RGO composite increases in comparison to the absorbance of the ZnO NPs. Such an increase in absorbance may be due to the absorption contribution from RGO, the increase in the surface electric charge of the oxides, and the modification of the fundamental process of electron–hole pair formation during irradiation [21]. Therefore, the presence of RGO in ZnO can increase the light absorption intensity and range, which is beneficial to the photocatalytic performance.

Fig. 5(a) illustrates the optical absorption spectra of the MB aqueous solution with 10 mg of the as-prepared ZnO-NPs/RGO composite after exposure to UV light irradiation for different intervals of times. It can be seen that the intensity of the absorption peak of MB at 663 nm decreases with an increase in the irradiation time, which indicates that the MB molecules are degraded by the catalysis. Fig. 5(b) shows the relative concentration (C_t/C_0) of MB as a function of time, where C_t is the concentration of MB at the irradiation time t, and C_0 is the concentration of the dye before irradiation. The result is plotted against those of the as-prepared ZnO-NPs/RGO and ZnO NPs under same conditions. The MB solution was degraded by as much as 99.5% by the ZnO-NPs/RGO and by approximately 63% by the ZnO NPs. This indicates the higher photocatalytic activity of the ZnO-NPs/RGO. In fact, the wide surface of RGO causes the ZnO NPs to disperse. Therefore, the dispersed NPs absorb more light and generate more electron–hole pairs to remove dye molecules.

4. Conclusion

ZnO-NPs/RGO was synthesized by the sol–gel method in a gelatin medium. FESEM and TEM images showed that the ZnO NPs were decorated and dispersed on the RGO. An HRTEM image of the NPs revealed that the ZnO NPs were single crystals without any defects. The XRD pattern of the ZnO-NPs/RGO indicated a hexagonal phase for the obtained product. The FTIR results showed that the post-annealing process removed the gelatin medium and formed the ZnO structure. In addition, the FTIR showed that the GO was transformed into RGO by the post-annealing process. The photocatalyst activity revealed the high MB removal efficiency of the ZnO-NPs/RGO in comparison to the ZnO NPs. This method can be used for the large-scale removal of pollutants from wastewater.

Acknowledgment

M. Azarang gratefully acknowledges the University of Malaya for its support in this research work by a research grant with No. PG058-2012B. In addition, A. Shuhaimi acknowledges obtaining a High Impact Research Grant University of Malaya Research Grant (UMRG: RP007B-13AFR). R. Yousefi acknowledges the Islamic Azad University, Masjed-Soleiman Branch, Iran.

References

[1] I. Arslan, I.A. Balcioglu, T. Tuhkanen, D. Bahnemann, H_2O_2/UV-C and Fe^{2+}/H_2O_2/UV-C versus TiO_2/UV-A treatment for reactive dye wastewater, J. Environ. Eng. 126 (2000) 903–911.
[2] E. Forgacs, T. Cserhati, G. Oros, Removal of synthetic dyes from wastewaters: a review, Environ. Int. 30 (2004) 953–971.
[3] M.R. Hoffmann, S.T. Martin, W.Y. Choi, O.W. Bahnemannt, Environmental applications of semiconductor photocatalysis, Chem. Rev. 95 (1995) 69–96.
[4] W. Yao, X. Fang, D.F. Guo, Z.Y. Gao, D.P. Wu, K. Jiang, Synthesis of ZnO/CdSe hierarchical heterostructure with improved visible photocatalytic efficiency, Appl. Surf. Sci. 274 (2013) 39–44.
[5] M.H. Huang, S. Mao, H. Feick, H. Yan, Y. Wu, H. Kind, E. Weber, R. Russo, P. Yang, Room-temperature ultraviolet nanowire nanolasers, Science 292 (2001) 1897–1899.
[6] S.J. Pearton, D.P. Norton, K. Ip, Y.W. Heo, T. Steiner, Recent progress in processing and properties of ZnO, Prog. Mater. Sci. 50 (2005) 293–340.
[7] T.J. Minami, Transparent and conductive multicomponent oxide films prepared by magnetron sputtering, J. Vac. Sci. Technol. A 17 (1999) 1765.
[8] A. Qurashi, M.F. Hossain, M. Faiz, N. Tabet, M.W. Alam, N.K. Reddy, Fabrication of well-aligned and dumbbell-shaped hexagonal ZnO nanorod arrays and their dye sensitized solar cell applications, J. Alloys Compd. 503 (2010) L40–L43.
[9] Y. Zong, Y. Cao, D. Jia, S. Bao, Y. Lu, Facile synthesis of Ag/ZnO nanorods using Ag/C cables as templates and their gas-sensing properties, Mater. Lett. 64 (2010) 243.
[10] R. Yousefi, F. Jamali-Sheini, M.R. Muhamad, M.A. More, Characterization and field emission properties of ZnMgO nanowires fabricated by thermal evaporation process, Solid State Sci. 12 (2010) 1088e1093.
[11] R.Y. Hong, J.H. Li, L.L. Chena, D.Q. Liua, H.Z. Li, Y. Zheng, J. Ding, Synthesis, surface modification and photocatalytic property of ZnO nanoparticles, Powder Technol. 189 (2009) 426–432.

[12] R. Yousefi, F. Jamali-Sheini, A. Khorsand Zak, M. Azarang, Growth and optical properties of ZnO–In_2O_3 heterostructure nanowires, Ceram. Int. 39 (2013) 5191–5196.
[13] O. Akhavan, E. Ghaderi, Toxicity of graphene and graphene oxide nanowalls against bacteria, ACS Nano 4 (10) (2010) 5731–5736.
[14] Likun Xinjuan Liu, Qingfei Pan, Tian Zhao, Guang Lv, Taiqiang Zhu, Ting Chen, Zhuo Lu, Changqing Sun, Sun, UV-assisted photocatalytic synthesis of ZnO-reduced graphene oxide composites with enhanced photocatalytic activity in reduction of Cr(VI), Chem. Eng. J. 183 (2012) 238–243.
[15] W.S. Hummers, R.E. Offeman, Preparation of graphitic oxide, J. Am. Chem. Soc. 80 (1958) 1339.
[16] J. Shen, B. Yan, M. Shi, H. Ma, N. Li, M. Ye, One step hydrothermal synthesis of TiO_2-reduced graphene oxide sheets, J. Mater. Chem. 21 (2011) 3415–3421.
[17] P.G. Ren, D.X. Yan, X. Ji, T. Chen, Z.M. Li, Temperature dependence of graphene oxide reduced by hydrazine hydrate, Nanotechnology 22 (2011) 055705.
[18] W. Zou, J. Zhu, Y. Sun, X. Wang, Depositing ZnO nanoparticles onto graphene in a polyol system, Mater. Chem. Phys. 125 (2011) 617–620.
[19] A. Khorsand Zak, W.H. Abd., M. Majid, R. Darroudi, Synthesis and characterization of ZnO nanoparticles prepared in gelatin media, Mater. Lett. 65 (2011) 70–73.
[20] A. Sáaedi, R. Yousefi, F. Jamali-Sheini, M. Cheraghizade, A. Khorsand Zak, N.M. Huang, Optical and electrical properties of p-type Li-doped ZnO nanowires, Superlattices Microstruct. 61 (2013) 91–96.
[21] T.G. Xu, L.W. Zhang, H.Y. Cheng, Y.F. Zhu, Significantly enhanced photocatalytic performance of ZnO via graphene hybridization and the mechanism study, Appl. Catal. B: Environ. 101 (2011) 382–387.